Preclinical validation of [18F]2FNQ1P as a specific PET radiotracer of 5-HT6 receptors in rat, pig, non-human primate and human brain tissue

Stéphane Emery, Sylvain Fieux, Benjamin Vidal, Pierre Courault, Sandrine Bouvard, Christian Tourvieille, Thibaut Iecker, Thierry Billard, Luc Zimmer, Sophie Lancelot

Preclinical validation of [^{18}F]2FNQ1P as a specific PET radiotracer of 5-HT$_6$ receptors in rat, pig, non-human primate and human brain tissue

Stéphane Emery[1,2], Sylvain Fieux[1], Benjamin Vidal[1], Pierre Courault[1,2], Sandrine Bouvard[1], Christian Tourvieille[3], Thibaut Iecker[3], Thierry Billard[3,4], Luc Zimmer[1,2,3,5*], Sophie Lancelot[1,2,3]

[1]Lyon Neuroscience Research Center, Université de Lyon, CNRS, INSERM, Lyon, France

[2]Hospices Civils de Lyon, Bron, France

[3]CERMEP Imaging Platform, Bron, France

[4]Institute of Chemistry and Biochemistry, Université de Lyon, CNRS, Villeurbanne, France

[5]National Institute for Nuclear Science and Technology INSTN, CEA, Saclay, France

Abbreviated title: [^{18}F]2FNQ1P, a 5-HT$_6$ PET radiotracer

Key words: PET radiotracer development; serotonin; 5-HT$_6$ receptor

*Corresponding author at: CERMEP, Groupement Hospitalier Est, 59 Boulevard Pinel, F-69003 Lyon, France; email address: luc.zimmer@univ-lyon1.fr (L. Zimmer)

Tel: +33(0)04 72 68 86 00; Fax: +33(0)04 72 68 86 10

Abstract

Introduction The aim of this study was to perform in-vitro and in -vivo radiopharmacological characterizations of [^{18}F]2FNQ1P, a new PET radiotracer of 5-HT$_6$ receptors, in rat, pig, non-human primate and human tissues. The 5-HT$_6$ receptor is one of the more recently identified serotonin receptors in central nervous system and, because of its role in memory and cognitive processes, is considered as a promising therapeutic target.

Methods In-vitro autoradiography and saturation binding assays were performed in postmortem brain tissues from rat, pig, non-human primate and human caudate nucleus, completed by serum stability assessment in all species and cerebral radiometabolite and biodistribution studies in rat.

Results In all species, autoradiography data revealed high binding levels of [^{18}F]2FNQ1P in cerebral regions with high 5-HT$_6$ receptor density. Binding was blocked by addition of SB258585 as a specific antagonist. Binding assays provided K_D and B_{max} values of respectively 1.34 nM and 0.03 pmol.mg^{-1} in rat, 0.60 nM and 0.04 pmol.mg^{-1} in pig, 1.38 nM and 0.07 pmol.mg^{-1} in non-human primate, and 1.39 nM and 0.15 pmol.mg^{-1} in human caudate nucleus. In rat brain, the proportion of unmetabolized [^{18}F]2FNQ1P was greater than 99% 5 minutes after iv injection and 89% at 40 minutes. The biodistribution studies found maximal radioactivity in lungs and kidneys (3.5 ± 1.2% ID/g and 2.0 ± 0.7% ID/g, respectively, 15 min post-injection).

Conclusion These radiopharmacological data confirm that [^{18}F]2FNQ1P is a specific radiotracer for molecular imaging of 5-HT$_6$ receptors and suggest that it could be used as a radiopharmaceutical in humans.

Introduction

Serotonin (5-HT) is a neurotransmitter involved in a variety of central nervous system (CNS) functions and behaviors, including sleep, cognitive processes, nociception, appetite and sexuality [1].

Serotonin receptor subtype-6 of (5-HT_6) is one of the more recently identified serotonin receptors, first in rat striatum [2,3] and then in human brain [4]. It is a G-protein-coupled receptor that has recently emerged as a new target for neuropsychopharmacology. 5-HT_6 receptor is expressed in the CNS, playing a vital role in memory and cognitive processes [5,6] and in the regulation of food intake [7,8], reinforcing its status as an emerging target in dementia and obesity therapy.

Distribution in humans is mainly in the striatum, but also prefrontal cortex and hippocampus [9,10]. It was also shown that the 5-HT_6 receptor is expressed at neuronal level in striatum, on astrocytes and pyramidal neurons of the cortex and on pyramidal neurons of the hippocampus. It therefore seems that the human 5-HT_6 receptor is expressed in different cell types depending on the brain region studied. 5-HT_6 receptors in the CNS are exclusively expressed in regions that play a key role in cognitive processes [11,12]. In preclinical studies, 5-HT_6 receptor antagonists were shown to improve cognitive performance [13,14]; recent clinical studies failed to confirm the pro-cognitive effects of 5-HT_6 antagonists idalopirdine and SAM-760in Alzheimer's disease [15,16], but other 5-HT_6 receptor antagonists are still being investigated, such as SUVN-502, currently in Phase II trials [17]. Paradoxically, 5-HT_6 receptor agonists have also been shown to have cognitive-enhancing properties [18,19].

In this context, the development of a new 5-HT_6 radiopharmaceutical for positron emission tomography (PET) seems relevant. PET is an imaging modality used in nuclear medicine to

study the function and neurochemistry of the human brain that relies on injection of a specific radiotracer [20–22]. PET provides incomparable molecular specificity and sensitivity in imaging, shedding light on pathophysiological mechanisms involving serotoninergic receptors or evaluating the pharmacological action of new drug candidates [23–26]. Several PET radiotracers have already been developed for serotonin receptor imaging, but there are as yet no in-vivo biomarkers that unequivocally distinguish serotonin receptor subtype 6. Some teams addressed this by synthesizing different compounds: [^{18}F]12ST05 is non-specific for 5HT$_6$R [27] and [^{11}C] GSK215083 is not selective (with affinity for 5-HT$_{2A}$) [28]. [^{11}C]399885 has low cerebral penetration [29], which makes it incompatible with peripheral injection. Currently, no specific fluorinated radiotracer is available for PET imaging of 5-HT$_6$ receptors in humans [30]. A specific radiotracer suitable for routine medical use could confirm 5-HT$_6$ receptor involvement in cognitive disorders and many pathologies [31], enabling monitoring of disease progression, to optimize future treatments. Our laboratory recently proposed a radiotracer-candidate, 2FNQ1P, inspired by the quinolone core of GSK215083 and proposed as the first ^{18}F-labeled radiotracer capable of specific and selective binding to 5HT$_6$R. In initial studies, the cerebral distribution of [^{18}F]2FNQ1P was analyzed in several animal models[23,32,33]. The present article completes the radiopharmacological and pharmacokinetics knowledge of [^{18}F]2FNQ1P and provides new experimental data obtained in postmortem rat, pig, non-human primate and human caudate tissues.

Materials and Methods

[^{18}F]2FNQ1P radiosynthesis

2FNQ1P precursor was synthesized in the Institute of Chemistry and Biochemistry (Lyon, France), and radiolabeling was performed in the radiopharmacy unit of the CERMEP imaging

platform, according to our recently published protocol [32,33]. Quality control consisted in determining radiochemical purity and molar activity by analytical HPLC assay of an aliquot of the radiolabeled product, with comparison to the calibration curve generated from solutions at known concentrations.

Drugs

Cyclosporin (Sandimmun®), used to inhibit the P-glycoprotein (P-gp), was obtained from Novartis. SB258585 hydrochloride, a 5-HT_6 serotonin receptor antagonist, was obtained from Sigma-Aldrich.

Animals and human tissues

Adult male Sprague-Dawley rats (Charles River Laboratories; 250g ± 50 g) and two pigs (30-35 kg) were used. Two healthy male cynomolgus monkeys (Macaca fascicularis), 4 and 5 years old (young adults) and weighing 4 and 7 kg respectively, were used. All studies were carried out in accordance with European Communities Council Directive (2°10/63/EU) and the recommendations of the French National Committee (2013/113) and local animal ethics committee (CELYNE, C2EA-43). For the in-vitro part of the study, following the "3Rs" rule (Reduction, Refinement, and Replacement) rule for animal experimentation, frozen tissues from previous studies were used [23,33].

Fresh tissues and adjacent unstained frozen slides (30µm-thickness) from healthy human caudates were obtained respectively from the Medical Research Council (Lyon) bank (CardioBioTec, Lyon Hospitals) and Medical Research Council (London) Neurodegenerative Diseases Brain Bank after approval by the hospital department's review committee.

In-vitro autoradiography

In-vitro autoradiography study was performed on brain tissues from rats (n=2), pigs (n=2), non-human primates (n=2) and human caudates (healthy controls, n=3). Briefly, adjacent 30 µm-coronal brain slices unfixed by paraformaldehyde were mounted on glass slides, and allowed to air-dry before storage at -80°C until use. On the day of radiotracer synthesis, the slides were allowed to reach room temperature and were then incubated for 60 min in a buffer containing 50 mM Tris-HCl, 10 µM pargyline, 5 mM $MgCl_2$, 5 mM ascorbate and 0.5 mM EDTA (pH 7.4), and 37 kBq/mL [^{18}F]2FNQ1P. For competition experiments, the slides were placed in the same buffer supplemented with SB258585 at a concentration of 1 µM. After incubation, slides were dipped in cold buffer (4°C), then in cold distilled water (4°C), and dried and placed on a phosphor imaging plate for 60 min (BAS-5000; Fujifilm).

In-vitro binding assays

Caudate tissues from adult rat (n=1), pig (n=2), non-human primate (n=1) and healthy controls (n=3) were used. Tissues were preserved in phosphate-buffered saline (PBS) EDTA 0.1% with buffer (50 mM Tris-HCl pH 7.4 at 25°C). Homogenates were centrifuged for 20 minutes at 35,000 g (Discovery M150 SE ultracentrifuge, Hitachi). The pellet was resuspended in 50 mM Tris-HCl (pH 7.4 at 25°C) and incubated for 15 minutes at 37°C. Following two further centrifugation steps (as above), the membranes were finally resuspended and stored at -80°C until use. Brain tissues were preserved in a buffer containing 50 mM Tris-HCl, 10 µM pargyline, 5 mM $MgCl_2$, 5 mM ascorbate and 0.5 mM EDTA (pH 7.4). Binding assay used 50 µL displacing compound (SB258585 1µM) or buffer, 100 µL membrane suspension (corresponding to approximately 60 µg protein per well of brain tissue) and 50 µL [^{18}F]2FNQ1P (molar activity, 59.2 GBq/µmol). [^{18}F]2FNQ1P was used at a

concentration of 0.05 to 10 nM. Membranes were incubated with the radioligand at 25°C for 60 minutes. Bound radiolabeled tracer was separated from free tracer by filtration under reduced pressure (Multiscreen HTS-FB, Millipore). Filters were washed 6 times with 200 µL PBS. Washed filters were assayed for radioactivity by γ-counter (Gamma Wizard 2480, Perkin Elmer).

Serum stability study

The serum stability study was carried out using a procedure similar to that described by Kronauge et al. [34]. In all species, 3.0-3.7 MBq of [^{18}F]2FNQ1P in 20 µL 10% ethanol/PBS was added to 200 µL of serum in a borosilicate culture tube equilibrated to 37°C in a water bath. The tubes were shaken and the samples were placed back in the water bath. At time points t=0 and t=2h, enzymatic hydrolysis was stopped by addition of cold (4°C) absolute ethanol (1 mL); the samples were cooled in an ice bath to precipitate serum proteins and centrifuged (15 min, 2500×g, 4°C), and the supernatant was analyzed by HPLC.

Brain metabolite analysis

Rats (n=2 per step) were anesthetized by intraperitoneal injection of urethane (1.25 g/kg) and a catheter was inserted in the caudal vein. The rats were pre-injected with cyclosporin (50 mg/kg i.v., 30 min prior to administration of ~~15.0 ± 0.5 mg~~ [^{18}F]2FNQ1P). The rats were killed by decapitation 5, 10, 20 or 40 min after bolus injection of [^{18}F]2FNQ1P (36 ± 2 MBq). The brains were carefully removed; each hemisphere was homogenized in 400 µL perchloric acid at 0.4 mol/L and centrifuged at 1,000 g for 10 min. The supernatant was neutralized by 120 µL 4 M potassium acetate and filtered (0.45 µm) before HPLC. The HPLC system consisted of a C-18 reversed phase column (C18 Nucleodur 5 µm, 4.6 × 250 mm column;

elution with H_3PO_4 (20 mM) 77%/THF 23%) at a flow rate of 0.9 mL.min^{-1}. During elution, 1-min fractions were collected and counted for radioactivity with an automated γ-counter (Gamma Wizard 2480, Perkin Elmer).

Biodistribution studies

Rats (n=4 per step) were anesthetized by intraperitoneal injection of urethane (1.25 g/kg) and a catheter was inserted in the caudal vein. 56 ± 19 MBq were injected per rats (represented 0.65 ± 0.22 nmol of radiotracer). Rats were euthanized at selected times up to 1 h after injection (15, 30, 45 min and 1h) by decapitation, and blood was immediately collected by cardiac puncture. Different samples from each rat were measured with a γ-counter (Gamma Wizard 2480, Perkin Elmer).

Data analysis

In radioligand binding studies, K_D and B_{max} values were calculated using GraphPad Prism software (Graph Pad Software, Prism 6). B_{max} values were expressed in pmol of [^{18}F]2FNQ1P per mg of protein. Data were expressed as mean ± standard error of mean (SEM) of at least three separate experiments.

Results

[^{18}F]2FNQ1P radiosynthesis and quality controls

Automated radiolabeling of 2FNQ1P leading to [^{18}F]2FNQ1P was performed from its nitro-precursor at 150°C in DMSO, on a Neptis synthesizer, with a radiochemical yield range of

25-36% corrected for decay and 72-78 min radiosynthesis time (including HPLC purification and formulation) (Fig.1). No radioactive by-products were observed and the HPLC conditions ensured good separation of the radiotracer from its nitro-precursor, as confirmed on quality control. Radiochemical purity was better than 99% and [^{18}F]2FNQ1P molar activity was between 264 and 372 GBq/µmol, corrected at end of synthesis.

In-vitro autoradiography

The autoradiography experiments revealed [^{18}F]2FNQ1P binding to various brain regions in postmortem tissues for all species (Fig. 2).

In rat and non-human primate, binding levels were especially high in the frontal cortex, cingulate cortex, basal ganglia, hippocampus and thalamus. In pig, binding levels were high in the frontal cortex and high-to-moderate in putamen and hippocampus. In these three species, binding levels were lower in other cortical regions. In human caudate, autoradiography data showed wide-scale binding. Uptake was ~~substancially~~ diminished from 20 to 40 % in all regions after competition with SB258585 at 1µM (Fig. 2). These results demonstrated the sensitivity of [^{18}F]2FNQ1P toward 5-HT$_6$ receptors.

In-vitro binding assays

[^{18}F]2FNQ1P bound with high affinity to 5-HT$_6$ receptors localized in various caudate membranes in rats, pigs, non-human primates and healthy controls. Saturation analysis of [^{18}F]2FNQ1P binding to native 5-HT$_6$ receptors revealed a single binding site in all species (Fig.3). Non-specific binding was shown in presence of SB258585 at 1 µM. Radioligand equilibrium dissociation constants (K_D) were 1.34 nM in rat, 0.60 ± 0.09 nM in pig, 1.38 nM

in non-human primate, and 1.39 ± 0.46 nM in healthy controls. Total receptor density (B_{max}) in the various tissues was 0.03 pmol.mg^{-1} in rat, 0.04 ± 0.01 pmol.mg^{-1} in pig, 0.07 pmol.mg^{-1} in non-human primate, and 0.15 ± 0.05 pmol.mg^{-1} in healthy controls. Examples of saturation binding curves and Scatchard plots are shown in Fig.3.

Serum stability study

The data clearly showed that [^{18}F]2FNQ1P was not hydrolyzed at t=2h in comparison with t=0 in rat, pig, non-human primate and human sera. Stability in human serum at each time point is seen in the chromatogram in Figure 4. As expected, there was no decomposition of the control sample in PBS.

Brain metabolite analysis

With pre-injection of cyclosporin, the radiochromatograms of brain activity in rat plasma at various times (5, 10, 20 and 40 min) after injection of [^{18}F]2FNQ1P showed negligible amounts of radioactive metabolite. The amount of radioactivity from unmetabolized [^{18}F]2FNQ1P was greater than 99.5% at 5 min and decreased to 98.8% at 10 min, 95.5% at 20 min and 88.6% at 40 min (Fig.5).

Biodistribution studies

The concentration of radioactivity in rat tissues (%ID/g) at selected times after i.v. injection of [^{18}F]2FNQ1P (44.5 ± 9 MBq) is shown Fig.6. Concentration was highest in the lungs (up to 3.5 ± 1.2%ID/g) and kidneys (up to 2.0 ± 0.7%ID/g) at 15 minutes post-injection, but decreased over a 60 minute period to 0.7 ± 0.1%ID/g and 0.9 ± 0.1%ID/g, respectively. The

next highest concentrations were in the spleen, liver and intestines (1.3 ± 0.1%ID/g, 1.2 ± 0.5 %ID/g, and 0.8 ± 0.2 %ID/g at 15 minutes post-injection, respectively), and were stable after 60 minutes. There was no accumulation of radioactivity in bone (0.3 to 0.2%ID/g). Uptake was low (≤ 0.1%ID/g) in the brains of healthy rats at all time points.

Discussion

There is currently no specific fluorinated antagonist of 5-HT_6 receptors available for clinical PET imaging. In this context, our team developed [^{18}F]2FNQ1P as the first 5-HT_6 antagonist PET radiotracer for imaging [33]. The initial strategy was to select [^{18}F]2FNQ1P for its 5-HT_6 receptor affinity and selectivity toward 5-HT_{2A} receptors, as determined on CHO cells [32]. It is now necessary to have more in-vitro data in order to better understand the characteristics of this radiopharmaceutical candidate, particularly with a view to future use in humans.

The present study systematically evaluated the pharmacokinetics of [^{18}F]2FNQ1P and explored its potential for PET imaging in different species and human tissues. Results confirmed that [^{18}F]2FNQ1P is a high-affinity reversible radioligand for 5-HT_6 receptors. In rat, pig, non-human primate brain and human caudate, autoradiography assay showed 5-HT_6 receptor distributions similar to those in the literature [35–37]. ~~The few differences in binding site concentrations in the present study may be attributable to the poorer resolution of the autoradiographic assay in comparison with immunohistochemistry.~~ To further confirm the binding specificity of [^{18}F]2FNQ1P for 5-HT_6 receptors, in-vitro displacement experiments were performed by treatment with unlabeled SB258585 as a selective 5-HT_6 receptor antagonist. A previous study had demonstrated that [^{125}I]SB258585 binding matched the brain

256 localization of 5-HT_6 receptors reasonably closely [38]. The present study showed strong
257 displacement, indicating high binding specificity of [^{18}F]2FNQ1P for 5-HT_6 receptors.

258 [^{18}F]2FNQ1P's high affinity for 5-HT_6 receptors was confirmed on in-vitro binding assay.
259 Pharmacokinetic analysis showed that [^{18}F]2FNQ1P binds with nanomolar affinity ($K_D \simeq 1$
260 nM) to a single binding site in membranes prepared from rat, pig, non-human primate and
261 healthy controls. These results confirmed those previously obtained with recombinant human
262 5-HT_6 receptors (Ki=0.9 nM) [32]. In addition, the binding site density in a sample of healthy
263 control caudate tissue was concordant with the 5-HT_6 receptor density reported in the
264 literature [38,39].

265 The pharmacological profile of [^{18}F]2FNQ1P as a novel 5-HT_6 receptor PET radiotracer did
266 not show any notable differences between rat, pig, non-human primate and human tissue,
267 suggesting that the radiopharmacological properties of the 5-HT_6 receptor are conserved
268 between species. The 5-HT_6 subtype is one of the most recently cloned serotonin receptors
269 [2,3,40], with 89% amino acid sequence homology between humans and rats [4]. In the serum
270 stability study, [^{18}F]2FNQ1P was stable in all species in vitro.

271 Brain metabolite analyses are a crucial step in the development of a new radiotracer. In the
272 case of [^{18}F]2FNQ1P, our previous study revealed a lack of brain penetration in the rat model
273 [33]. We proposed that blood-brain P-gp interacts with [^{18}F]2FNQ1P and strongly regulates
274 its brain penetration [41]. The lack of brain penetration in the rodent model is not
275 disqualifying for future radiopharmaceutical application, given the evidence of good brain
276 penetration in larger animals, including non-human primates [20,23,33]. It was nevertheless
277 useful to check whether the radiotracer tends to be found in metabolized form in the brain.
278 Because of the invasiveness of ex-vivo measurement in brain tissue, this approach can only be
279 used in small animals. We therefore pretreated rats with cyclosporin, used here as a P-gp

inhibitor [41], in order to reach a significant concentration of [^{18}F]2FNQ1P in the brain. The amount of total radioactivity was found to correspond mainly to unmetabolized [^{18}F]2FNQ1P, even at the latest time point of 40 min post-injection, ruling out any significant contribution of radiometabolites to brain uptake. These results showed that [^{18}F]2FNQ1P is also very stable in the brain, more than 88% being intact even 40 min after probe injection. This indicates that [^{18}F]2FNQ1P radiometabolites in plasma do not greatly cross the BBB, a characteristic favourable to the specificity of brain targeting.

In the whole body biodistribution study, the bone radioactivity accumulation of a fluorinated radiotracer is a very sensitive index of defluorination [42,43]. In the present case, there was no in-vivo bone accumulation of radioactivity between 15 and 60 minutes post-injection (0.29 to 0.16% ID/g). Biodistribution studies highlighted tissue-dependent [^{18}F]2FNQ1P accumulation rates. The highest radioactivity concentrations were found in kidney and liver, probably due to their involvement in the metabolism and excretion of the injected exogenous compound. Tracer fixation in lung can be explained by the presence of 5-HT$_6$ receptors in this organ. A study demonstrated high expression of 5-HT$_6$ receptors in the murine airway, tracheal muscle, main bronchus and lung [44]; the brain showed a very low tissue concentration, confirming that [^{18}F]2FNQ1P was not able to penetrate rat brain (0.11 to 0.05%ID/g).

Finally, these encouraging results, added to those of a previous PET study in non-human primate [23], confirm the selectivity of [^{18}F]2FNQ1P toward 5-HT$_6$ receptors and reinforce the idea that this radiotracer has a pharmacological profile suitable for in-vivo study in humans. [^{18}F]2FNQ1P could be useful tool for studying 5-HT$_6$ receptor density and distribution in animal disease models and in human brains from patients suffering from schizophrenia or Alzheimer's disease.

Conclusions

The interest of the development of a new PET radiotracer for 5-HT_6 receptors no longer needs to be demonstrated [45]. According to the experimental data available on [^{18}F]2FNQ1P, it may be useful for imaging 5-HT_6 receptors. The present study described the characterization of [^{18}F]2FNQ1P, which selectively binds to native 5-HT_6 receptors with high affinity. Future experiments, such as in-vivo radiometabolite analyses with input functions and imaging studies in non-human primates or humans, should demonstrate the suitability of [^{18}F]2FNQ1P as a new PET radiotracer.

Acknowledgments

We thank particularly David Meyronet and Anthony Fourier for the provision of human tissues.

Funding

This work was supported by a national Alzheimer Foundation grant 2016 (Fondation Alzheimer, France).

Conflict of Interest Statement

The authors declared no potential conflicts of interest with respect to the research, authorship, and/or publication of this article.

Bibliography

[1] Berger M, Gray JA, Roth BL. The expanded biology of serotonin. Annu Rev Med 2009;60:355-66.

[2] Monsma FJ, Shen Y, Ward RP, Hamblin MW, Sibley DR. Cloning and expression of a novel serotonin receptor with high affinity for tricyclic psychotropic drugs. Mol Pharmacol 1993;43:320-7.

[3] Ruat M, Traiffort E, Arrang JM, Tardivel-Lacombe J, Diaz J, Leurs R, et al. A novel rat serotonin (5-HT6) receptor: molecular cloning, localization and stimulation of cAMP accumulation. Biochem Biophys Res Commun 1993;193:268-76.

[4] Kohen R, Metcalf MA, Khan N, Druck T, Huebner K, Lachowicz JE, et al. Cloning, characterization, and chromosomal localization of a human 5-HT6 serotonin receptor. J Neurochem 1996;66:47-56.

[5] Mitchell ES. 5-HT6 receptor ligands as antidementia drugs. Int Rev Neurobiol 2011;96:163-87.

[6] Quiedeville A, Boulouard M, Da Silva Costa-Aze V, Dauphin F, Bouet V, Freret T. 5-HT6 receptor antagonists as treatment for age-related cognitive decline. Rev Neurosci 2014;25:417-27.

[7] Heal D, Gosden J, Smith S. The 5-HT6 receptor as a target for developing novel antiobesity drugs. Int Rev Neurobiol 2011;96:73-109.

[8] Kotańska M, Lustyk K, Bucki A, Marcinkowska M, Śniecikowska J, Kołaczkowski M. Idalopirdine, a selective 5-HT6 receptor antagonist, reduces food intake and body weight in a model of excessive eating. Metab Brain Dis 2018;33:733-40.

[9] Marazziti D, Baroni S, Pirone A, Giannaccini G, Betti L, Schmid L, et al. Distribution

of serotonin receptor of type 6 (5-HT_6) in human brain post-mortem. A pharmacology, autoradiography and immunohistochemistry study. Neurochem Res 2012;37:920-7.

[10] Marazziti D, Baroni S, Pirone A, Giannaccini G, Betti L, Testa G, et al. Serotonin receptor of type 6 (5-HT6) in human prefrontal cortex and hippocampus post-mortem: an immunohistochemical and immunofluorescence study. Neurochem Int 2013;62:182-8.

[11] Ramirez MJ, Lai MKP, Tordera RM, Francis PT. Serotonergic therapies for cognitive symptoms in Alzheimer's disease: rationale and current status. Drugs 2014;74:729-36.

[12] Meneses A, Pérez-García G, Ponce-Lopez T, Castillo C. 5-HT6 receptor memory and amnesia: behavioral pharmacology--learning and memory processes. Int Rev Neurobiol 2011;96:27-47.

[13] Arnt J, Bang-Andersen B, Grayson B, Bymaster FP, Cohen MP, DeLapp NW, et al. Lu AE58054, a 5-HT6 antagonist, reverses cognitive impairment induced by subchronic phencyclidine in a novel object recognition test in rats. Int J Neuropsychopharmacol 2010;13:1021-33.

[14] Callaghan CK, Hok V, Della-Chiesa A, Virley DJ, Upton N, O'Mara SM. Age-related declines in delayed non-match-to-sample performance (DNMS) are reversed by the novel 5HT6 receptor antagonist SB742457. Neuropharmacology 2012;63:890-7.

[15] Bennett DA. Lack of Benefit With Idalopirdine for Alzheimer Disease: Another Therapeutic Failure in a Complex Disease Process. JAMA 2018;319:123-5.

[16] Fullerton T, Binneman B, David W, Delnomdedieu M, Kupiec J, Lockwood P, et al. A Phase 2 clinical trial of PF-05212377 (SAM-760) in subjects with mild to moderate Alzheimer's disease with existing neuropsychiatric symptoms on a stable daily dose of donepezil. Alzheimers Res Ther 2018;10:38. https://doi.org/10.1186/s13195-018-0368-9.

[17] Nirogi R, Abraham R, Benade V, Medapati RB, Jayarajan P, Bhyrapuneni G, et al. SUVN-502, a novel, potent, pure, and orally active 5-HT6 receptor antagonist: pharmacological, behavioral, and neurochemical characterization. Behav Pharmacol 2019;30:16-35.

[18] Vanda D, Soural M, Canale V, Chaumont-Dubel S, Satała G, Kos T, et al. Novel non-sulfonamide 5-HT6 receptor partial inverse agonist in a group of imidazo[4,5-b]pyridines with cognition enhancing properties. Eur J Med Chem 2018;144:716-29.

[19] Karila D, Freret T, Bouet V, Boulouard M, Dallemagne P, Rochais C. Therapeutic Potential of 5-HT6 Receptor Agonists. J Med Chem 2015;58:7901-12.

[20] Zimmer L, Luxen A. PET radiotracers for molecular imaging in the brain: past, present and future. Neuroimage 2012;61:363-70.

[21] Cai W. Positron Emission Tomography: State of the Art. Mol Pharmaceutics 2014;11:3773-6.

[22] Ametamey SM, Honer M, Schubiger PA. Molecular Imaging with PET. Chem Rev 2008;108:1501-16.

[23] Sgambato-Faure V, Billard T, Météreau E, Duperrier S, Fieux S, Costes N, et al. Characterization and Reliability of [18F]2FNQ1P in Cynomolgus Monkeys as a PET Radiotracer for Serotonin 5-HT6 Receptors. Front Pharmacol 2017;8:471. https://doi.org/10.3389/fphar.2017.00471.

[24] Wagner CC, Langer O. Approaches using molecular imaging technology — use of PET in clinical microdose studies. Advanced Drug Delivery Reviews 2011;63:539-46.

[25] Chakravarty R, Hong H, Cai W. Positron Emission Tomography Image-Guided Drug Delivery: Current Status and Future Perspectives. Mol Pharmaceutics 2014;11:3777-97.

[26] Willmann JK, van Bruggen N, Dinkelborg LM, Gambhir SS. Molecular imaging in drug development. Nature Reviews Drug Discovery 2008;7:591-607.

[27] Tang S, Verdurand M, Joseph B, Lemoine L, Daoust A, Billard T, et al. Synthesis and biological evaluation in rat and cat of [18F]12ST05 as a potential 5-HT6 PET radioligand. Nucl Med Biol 2007;34:995-1002.

[28] Parker CA, Gunn RN, Rabiner EA, Slifstein M, Comley R, Salinas C, et al. Radiosynthesis and characterization of 11C-GSK215083 as a PET radioligand for the 5-HT6 receptor. J Nucl Med 2012;53:295-303.

[29] Liu F, Majo VJ, Prabhakaran J, Milak MS, John Mann J, Parsey RV, et al. Synthesis and in vivo evaluation of [O-methyl-11C] N-[3,5-dichloro-2-(methoxy)phenyl]-4-(methoxy)-3-(1-piperazinyl)benzenesulfonamide as an imaging probe for 5-HT6 receptors. Bioorg Med Chem 2011;19:5255-9.

[30] Billard T, Liger F, Verdurand M. Serotonin receptor imaging by 18F-PET. Fluorine in Life Sciences: Pharmaceuticals, Medicinal Diagnostics, and Agrochemicals, Elsevier; 2019, p. 459-518.

[31] Meneses A. Neural activity, memory, and dementias: serotonergic markers. Behav Pharmacol 2017;28:132-41.

[32] Colomb J, Becker G, Fieux S, Zimmer L, Billard T. Syntheses, radiolabelings, and in vitro evaluations of fluorinated PET radioligands of 5-HT6 serotoninergic receptors. J Med Chem 2014;57:3884-90.

[33] Becker G, Colomb J, Sgambato-Faure V, Tremblay L, Billard T, Zimmer L. Preclinical evaluation of [18F]2FNQ1P as the first fluorinated serotonin 5-HT6 radioligand for PET imaging. Eur J Nucl Med Mol Imaging 2015;42:495-502.

417 [34] Kronauge JF, Noska MA, Davison A, Holman BL, Jones AG. Interspecies variation in
418 biodistribution of technetium (2-carbomethoxy-2-isocyanopropane)6+. J Nucl Med
419 1992;33:1357-65.

420 [35] Chopra A. [11C]-[N-Methyl]3-[(3-fluorophenyl)sulfonyl]-8-(4-methyl-1-
421 piperazinyl)quinoline. Molecular Imaging and Contrast Agent Database (MICAD), Bethesda
422 (MD): National Center for Biotechnology Information (US); 2004.

423 [36] Witten L, Bang-Andersen B, Nielsen SM, Miller S, Christoffersen CT, Stensbøl TB, et
424 al. Characterization of [^{3}H]Lu AE60157 ([^{3}H]8-(4-methylpiperazin-1-yl)-3-
425 phenylsulfonylquinoline) binding to 5-hydroxytryptamine$_{6}$ (5-HT$_{6}$) receptors in vivo. Eur J
426 Pharmacol 2012;676:6-11.

427 [37] East SZ, Burnet PWJ, Leslie RA, Roberts JC, Harrison PJ. 5-HT6 receptor binding
428 sites in schizophrenia and following antipsychotic drug administration: autoradiographic
429 studies with [125I]SB-258585. Synapse 2002;45:191-9.

430 [38] Hirst WD, Minton JA, Bromidge SM, Moss SF, Latter AJ, Riley G, et al.
431 Characterization of [(125)I]-SB-258585 binding to human recombinant and native 5-HT(6)
432 receptors in rat, pig and human brain tissue. Br J Pharmacol 2000;130:1597-605.

433 [39] Boess FG, Riemer C, Bös M, Bentley J, Bourson A, Sleight AJ. The 5-
434 hydroxytryptamine6 receptor-selective radioligand [3H]Ro 63-0563 labels 5-
435 hydroxytryptamine receptor binding sites in rat and porcine striatum. Mol Pharmacol
436 1998;54:577-83.

437 [40] Woolley ML, Marsden CA, Fone KCF. 5-ht6 receptors. Curr Drug Targets CNS
438 Neurol Disord 2004;3:59-79.

439 [41] Laćan G, Plenevaux A, Rubins DJ, Way BM, Defraiteur C, Lemaire C, et al.

Cyclosporine, a P-glycoprotein modulator, increases [18F]MPPF uptake in rat brain and peripheral tissues: microPET and ex vivo studies. Eur J Nucl Med Mol Imaging 2008;35:2256-66.

[42] Berger F, Lee Y-P, Loening AM, Chatziioannou A, Freedland SJ, Leahy R, et al. Whole-body skeletal imaging in mice utilizing microPET: optimization of reproducibility and applications in animal models of bone disease. Eur J Nucl Med Mol Imaging 2002;29:1225-36.

[43] Blau M, Ganatra R, Bender MA. 18 F-fluoride for bone imaging. Semin Nucl Med 1972;2:31-7.

[44] Keshavarz M, Schwarz H, Hartmann P, Wiegand S, Skill M, Althaus M, et al. Caveolin-1: Functional Insights into Its Role in Muscarine- and Serotonin-Induced Smooth Muscle Constriction in Murine Airways. Front Physiol 2017;8:295. https://doi.org/10.3389/fphys.2017.00295.

[45] Khoury R, Grysman N, Gold J, Patel K, Grossberg GT. The role of 5 HT6-receptor antagonists in Alzheimer's disease: an update. Expert Opin Investig Drugs 2018;27:523-33.

Fig. 1. Synthesis of [^{18}F]2FNQ1P

Fig. 2. Representative in-vitro autoradiograms of [^{18}F]2FNQ1P binding in rat (A), pig (B), non-human primate (C) and human brain tissues (D) (sagittal brain sections for pig, coronal brain sections for rat and non-human primate, and caudate sections for healthy controls). [^{18}F]2FNQ1P distribution in cerebral regions was processed under baseline condition (total binding) and in presence of cold SB258585 (non-specific binding) (at 1µM). Arrows show frontal cortex (FC), cingulate cortex (Cg), caudate (Cd), putamen (Pu) and hippocampus (HIP).

Fig. 3. In-vitro binding assays in rat (A), pig (B), non-human primate (C), and human caudate (D). Examples of saturation binding curves and Scatchard plots of [^{18}F]2FNQ1P binding to caudate membrane.

Fig. 4. Human serum stability. HPLC analysis of [^{18}F]2FNQ1P following in-vitro incubation at 37°C at t=0 (red curve) and at t= 2h (blue curve) showed radiotracer stability for up to 2h in human serum.

Fig.5. Brain metabolite analysis. Radiochromatogram of radioactivity from 5 to 40 min after intravenous pre-injection of cyclosporin and injection of [^{18}F]2FNQ1P in rat. The main amount of radioactivity was eluted between 6 and 7 min, corresponding to the unmetabolized radiotracer (n=2).

Fig.6. Biodistribution of [^{18}F]2FNQ1P in rat at selected times up to 1 h after i.v. injection (tail vein) expressed as percentage injected dose per gram of tissue (%ID/g, mean and standard deviation, n=4).

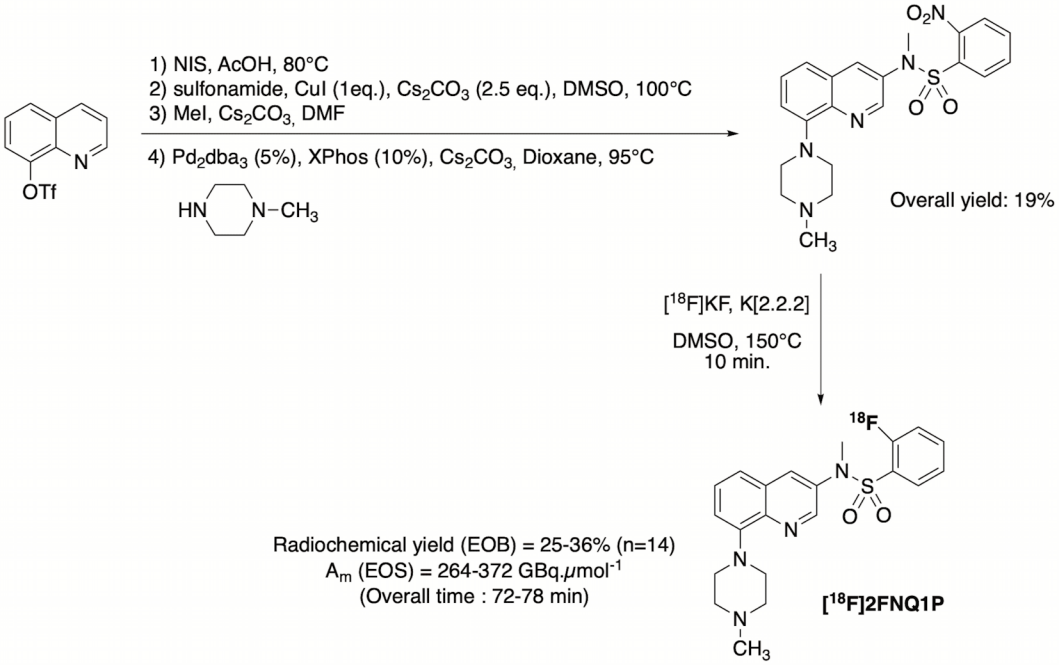
1) NIS, AcOH, 80°C
2) sulfonamide, CuI (1eq.), Cs_2CO_3 (2.5 eq.), DMSO, 100°C
3) MeI, Cs_2CO_3, DMF
4) Pd_2dba_3 (5%), XPhos (10%), Cs_2CO_3, Dioxane, 95°C
OTf
HN
N−CH3
O_2N
Overall yield: 19%
[18F]KF, K[2.2.2]
DMSO, 150°C
10 min.
18F
Radiochemical yield (EOB) = 25-36% (n=14)
A_m (EOS) = 264-372 GBq.μmol-1
(Overall time : 72-78 min)
[18F]2FNQ1P

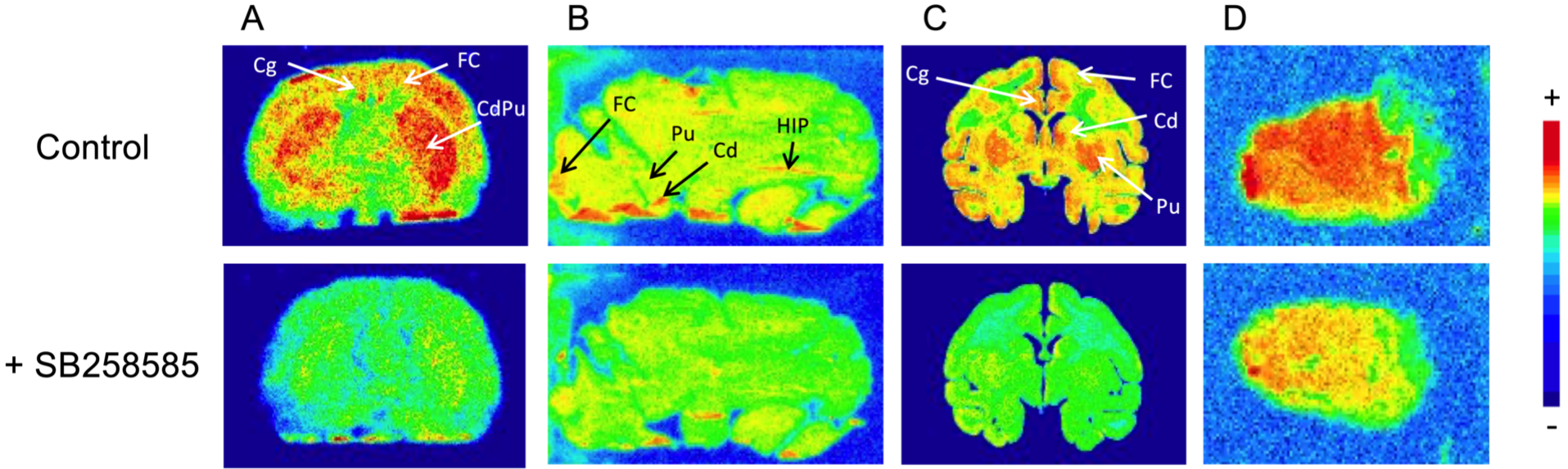
A
B
C
D
Control
+ SB258585
Cg
FC
CdPu
FC
Pu
Cd
HIP
Cg
FC
Cd
Pu
+
-

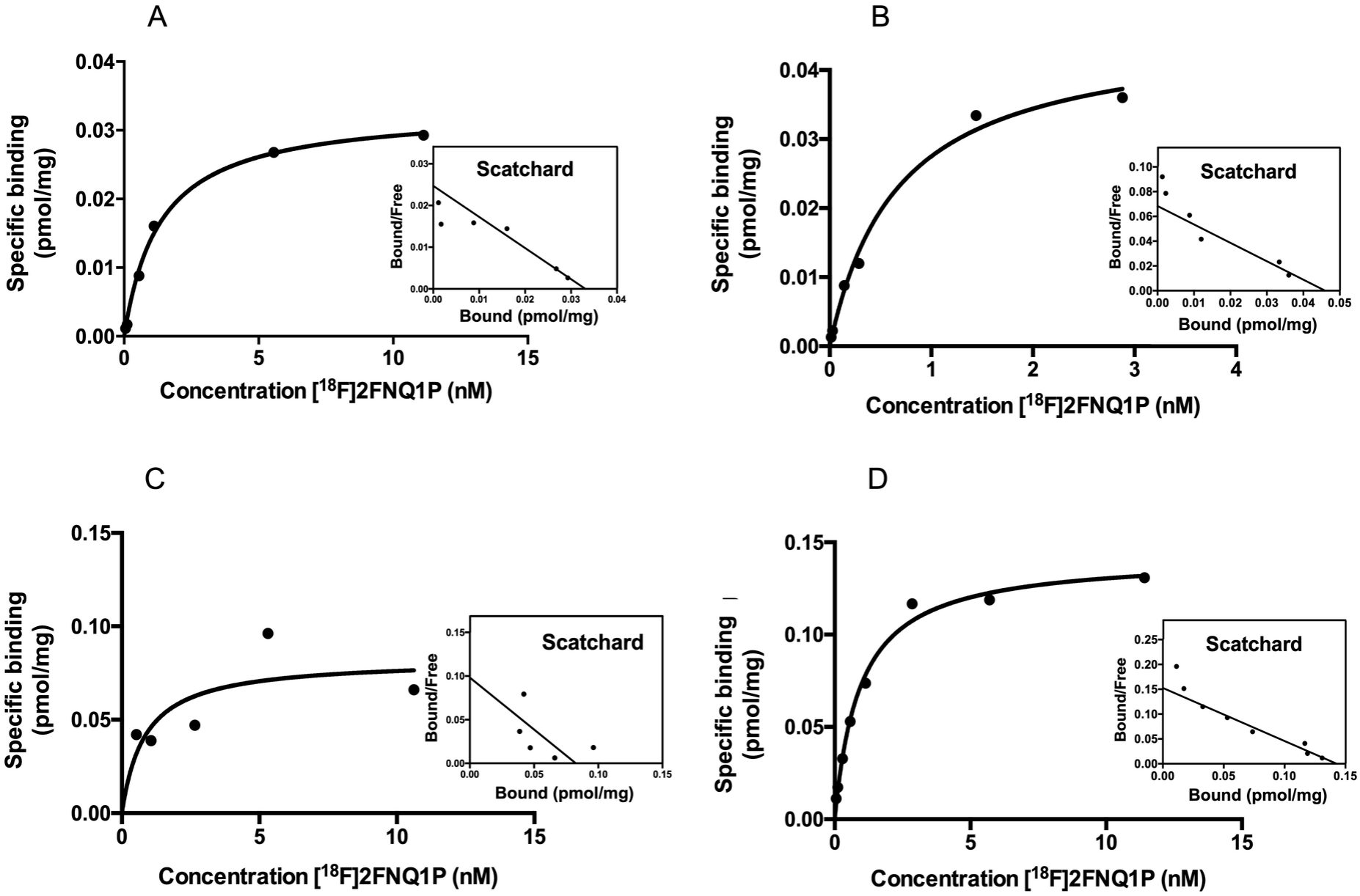
A
Specific binding (pmol/mg)
0.04
0.03
0.02
0.01
0.00
0
5
10
15
Concentration [18F]2FNQ1P (nM)
Scatchard
Bound/Free
Bound (pmol/mg)
B
Specific binding (pmol/mg)
0.04
0.03
0.02
0.01
0.00
0
1
2
3
4
Concentration [18F]2FNQ1P (nM)
Scatchard
Bound/Free
Bound (pmol/mg)
C
Specific binding (pmol/mg)
0.15
0.10
0.05
0.00
0
5
10
15
Concentration [18F]2FNQ1P (nM)
Scatchard
Bound/Free
Bound (pmol/mg)
D
Specific binding (pmol/mg)
0.15
0.10
0.05
0.00
0
5
10
15
Concentration [18F]2FNQ1P (nM)
Scatchard
Bound/Free
Bound (pmol/mg)

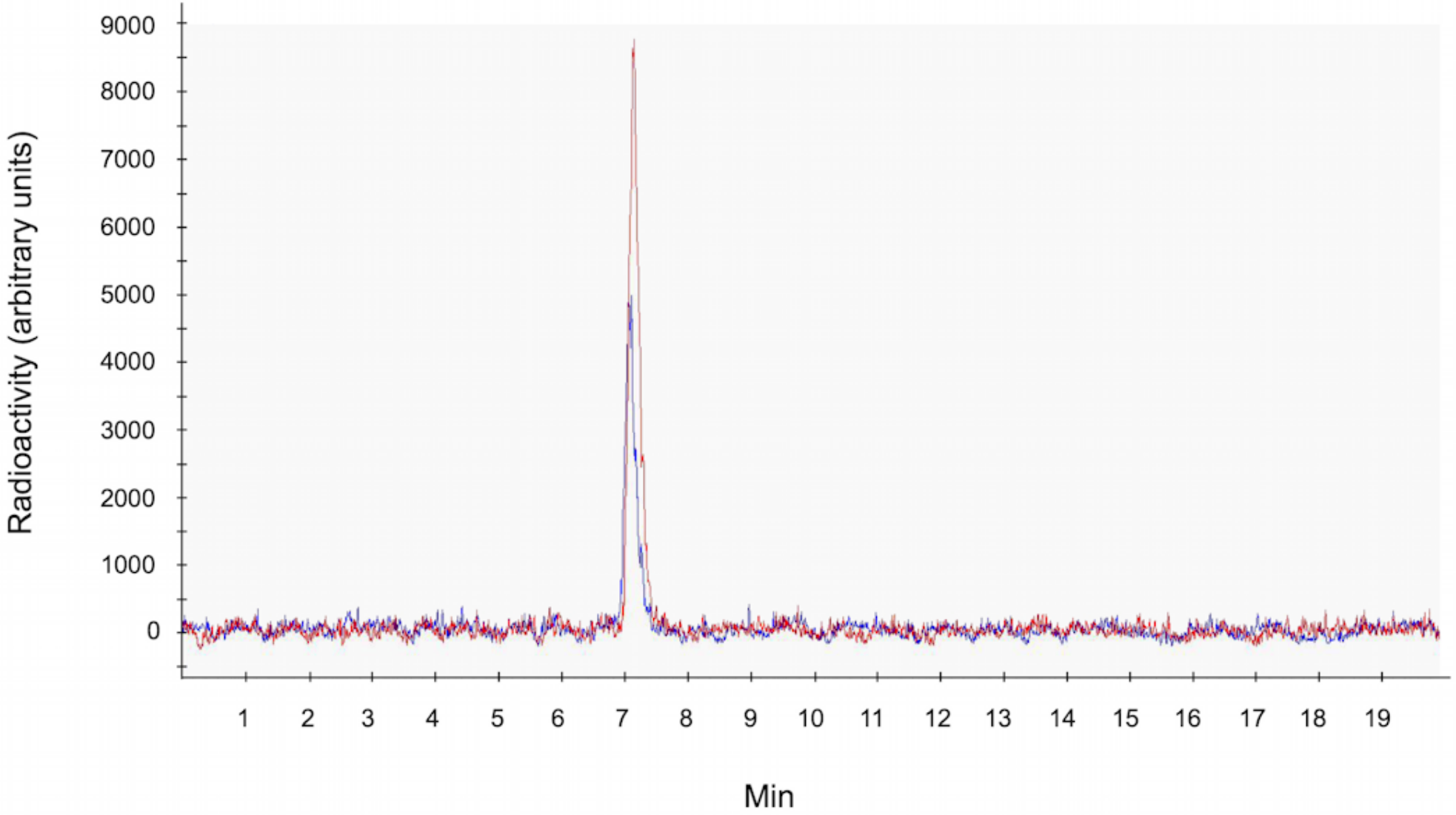
Radioactivity (arbitrary units)
9000
8000
7000
6000
5000
4000
3000
2000
1000
0
1
2
3
4
5
6
7
8
9
10
11
12
13
14
15
16
17
18
19
Min

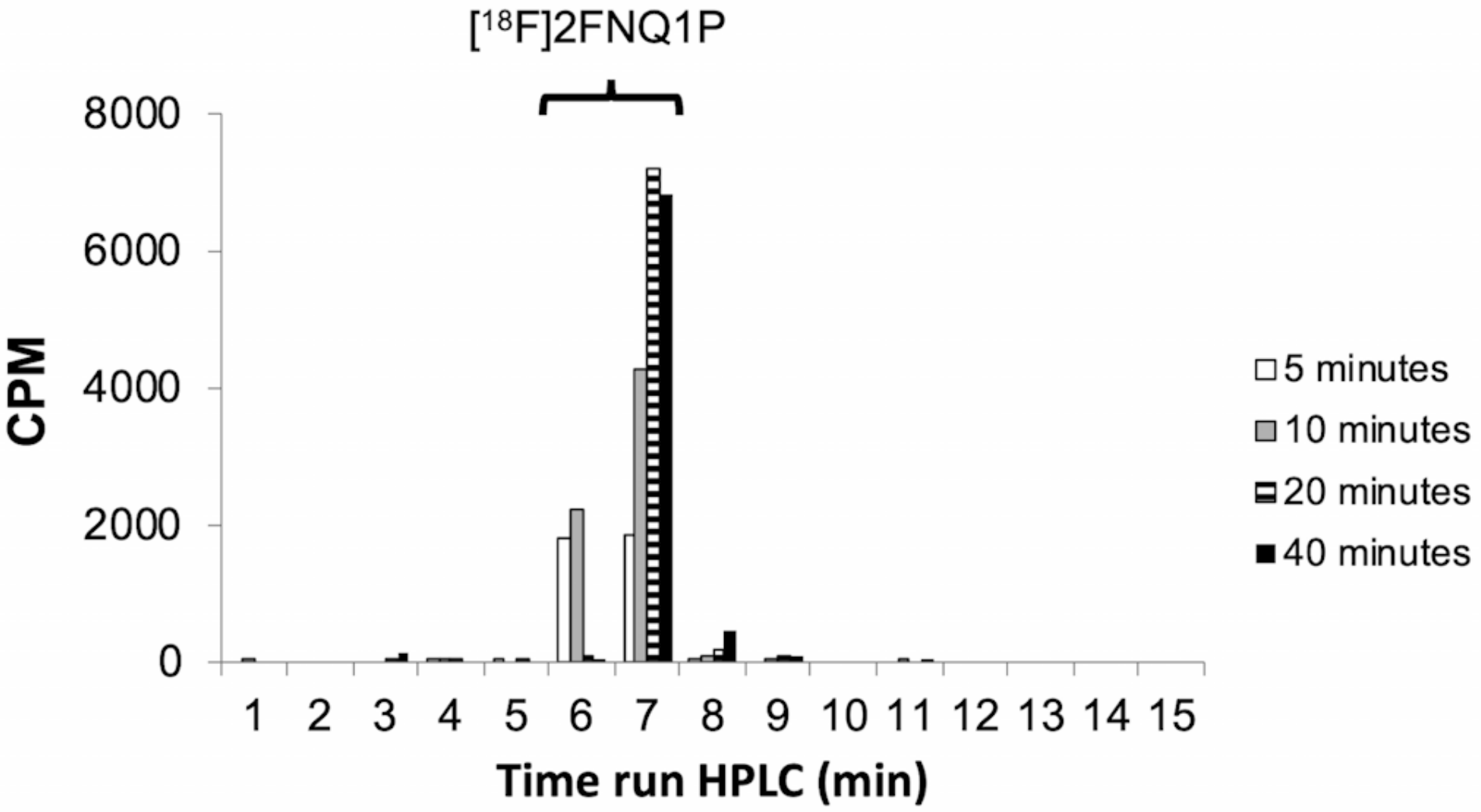
[18F]2FNQ1P
8000
6000
4000
2000
0
CPM
1 2 3 4 5 6 7 8 9 10 11 12 13 14 15
Time run HPLC (min)
5 minutes
10 minutes
20 minutes
40 minutes

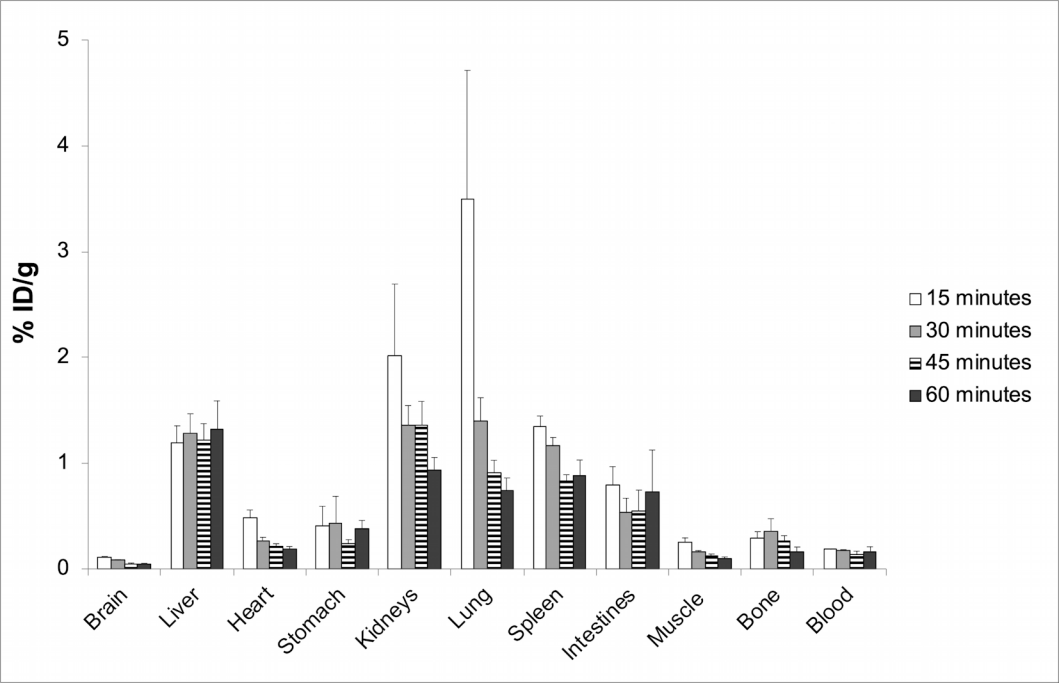
% ID/g
5
4
3
2
1
0
15 minutes
30 minutes
45 minutes
60 minutes
Brain
Liver
Heart
Stomach
Kidneys
Lung
Spleen
Intestines
Muscle
Bone
Blood